Defence Science Journal, Vol. 58, No. 2, March 2008, pp. 285-294

Brittle Failure in Heterogeneous Crystalline Rocks

K.S. Rao[1] and Hossein Noferesti[2]

[1]*Indian Institute of Technology Delhi, New Delhi-110 016*
[2]*Faculty of Engineering, University of Birjand, Birjand, Iran*

ABSTRACT

In a novel attempt to go further in details of the brittle failure process, an extensive study covering both experimental and numerical aspects, has been performed at the Indian Institute of Technology Delhi. Dental plaster has been selected as the base model material to simulate the natural conditions. The specimens were tested in biaxial loading condition after proper curing. To numerically simulate the problem, the UDEC software was used and the effect of geometrical heterogeneity has been studied. A failure criterion is proposed based upon this study.

Keywords: Brittle failure, crystalline rocks, microcracks, heterogeneity, dental plaster

NOMENCLATURE

σ_c	Uniaxial compressive strength
σ_{tm}	Tensile strength of rock minerals
E	Elastic modulus
E_m	Elastic modulus of rock minerals
v	Poisson's ratio
k	Static bulk modulus
K	Interlocking factor of minerals/grains/crystals
H	Vickers hardness number of a material
β	Angle between the sample surface and the indenter facet
SG	Specific gravity
γ_d	Dry density
n	Porosity
σ_t	Brazilian strength
c	Cohesion
$\varphi°$	Internal friction angle
k_y	Material constant
σ_0	Starting stress for dislocation movement
D	Average size of elements
ΔD_{av}	Difference between two sizes present in the system
L_{max}/L_{min}	Length ratio

1. INTRODUCTION

Brittle failure is the paramount type of failure occurring in rocks involving civil and mining engineering works. In spite of significant developments in rock mechanics in the recent past, sufficient insight into the real mechanism of brittle failure has not been achieved.

Received 30 October 2007

Crystalline rocks are a major group of rocks, including most igneous and metamorphic rocks, whose structure is made of mineral crystals interlocked together[1] (Fig. 1). Microscopic observations have proved that no chemical bond exists between crystals and that the overall strength of these rocks is owing to their very intricate and 3-D interlocking only[2] (Fig. 2). Considering the fact that most of the crystalline rocks are igneous, they were focused in further detail in this paper.

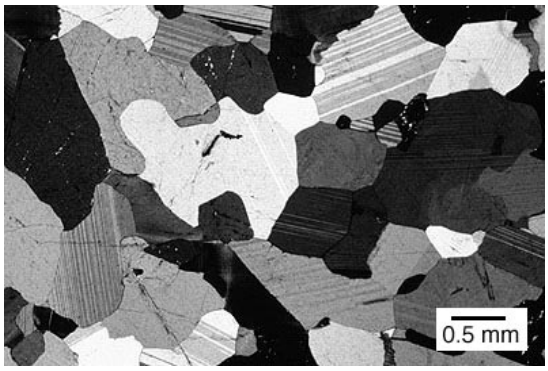

(a)

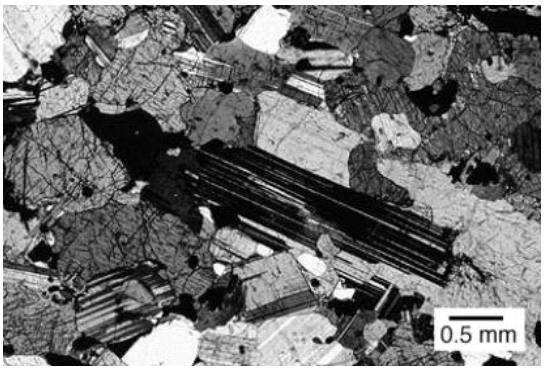

(b)

Figure 1. Interlocking textures of: (a) a metamorphic rock and (b) an igneous rock[1].

2. CHARACTERISTICS OF CRYSTALLINE ROCKS

In almost all igneous rocks, five major minerals, i.e., quartz, feldspar, mica, pyroxene, and olivine are present; the percentage of other minerals is negligible[3]. Attempts were made in the present study to simulate these minerals through suitable model materials. The ratios between uniaxial compressive strength, σ_c, and elastic modulus, E, of minerals were considered as the simulation parameters. The

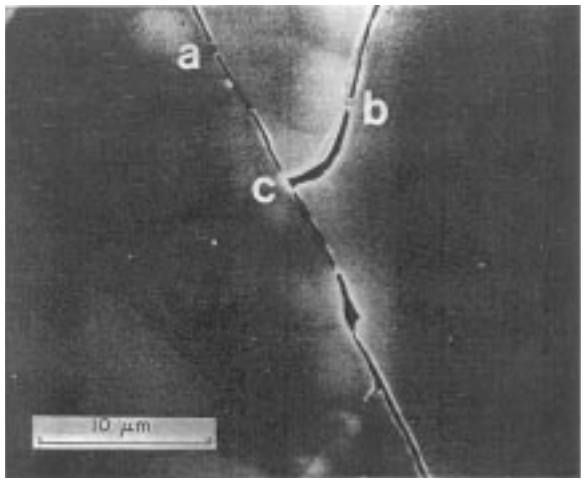

Figure 2. Quartz grain boundaries in westerly granite. a, b, and c refer to small bridges in the boundary cracks due to alteration or healing[2].

next step is to find their respective values. Having Poisson's ratio (v) from Belikov studies[4] and static bulk modulus (k) of minerals from Knittle[5], it is possible to estimate the E values in Table 1 from the following:

$$E = 3k(1-2v) \tag{1}$$

To calculate σ_c is further complicated, the indirect method adopted by Dorner and Stöckhert[6] is adopted here. In this method[7], having Vickers hardness number of a material, H, one can estimate σ_c using the following formula:

$$H = \frac{2}{3}\left\{2 + \ln\left[\frac{E\tan\beta}{6\sigma_c(1-v)} + \frac{2(1-2v)}{3(1-v)}\right]\right\}\sigma_c \tag{2}$$

Having hardness numbers of minerals[8] and using Eqn (2), σ_c values for five major minerals are calculated and presented in Table 1.

3. SELECTION AND CHARACTERISATION OF MODEL MATERIALS

To find out a suitable set of compositions capable of simulating the same ratios of strength and modulus as exists in five major minerals of igneous rocks, a variety of materials were considered. After a wide-ranging review and testing of natural and industrial materials, four varieties of dental plaster

Table 1. Average mechanical properties of major minerals present in igneous rocks

Mineral	E (GPa)	σ_c (GPa)	E/E_{Quartz}	$\sigma_c/\sigma_{cQuartz}$
Quartz	92.1	6.35	1.00	1.00
Olivine	195	4.11	2.25	0.65
Plagioclase	108.2	4.30	0.83	0.66
Alkali feldspar	84.4	4.14		
Pyroxene	187.2	2.86	1.55	0.45
Mica	81.2	0.33	0.72	0.05

are selected as model materials. Dental plasters are especially manufactured and extremely purified types of plaster of Paris that show remarkably high strength and modulus values. After final selection of four types of model materials, a detailed characterisation program was conducted to find out their exact physical and mechanical properties for future use in the main experimental program and analysis thereupon.

Specific gravity (SG), dry density, (γ_d), and porosity (n), as physical properties and uniaxial compressive strength (σ_c), Brazilian strength (σ_t), elastic modulus (E), Poisson's ratio (ν), cohesion (c), and internal friction angle, (φ^o), as mechanical properties were determined for all model materials with respect to the procedures suggested by ISRM[9,10] (Table 2). In Table 2, Q and B represent model materials quartz and biotite, respectively. Only single material, named as F, is selected to represent both feldspar and olivine since their strength ratios are same but olivine modulus ratio is too high and could not be achieved. In case of pyroxene and amphibole, material P is selected to represent both since their strength and modulus ratios are nearly same.

The complete stress-strain curves of four model materials are obtained as shown in Fig. 3. These curves resemble the stress-strain behaviour of brittle rocks with linear loading portions and sharp unloading portions, therefore further proving their suitability for use as a brittle model material.

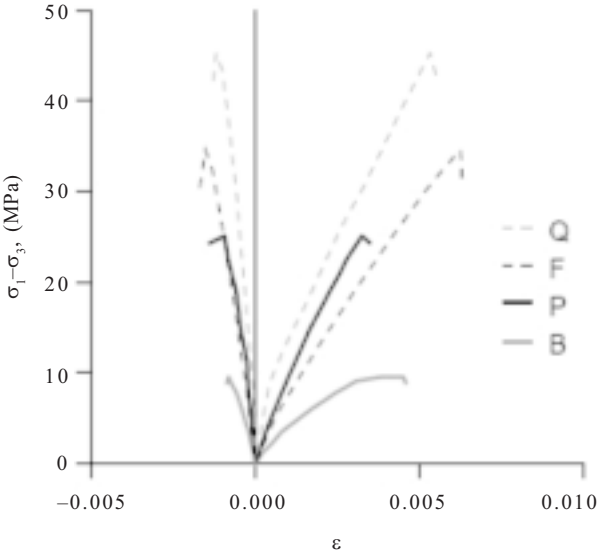

Figure 3. Stress-strain curves of four model materials.

Properties like shear and normal stiffness of interfaces between different types of model materials are determined, as well, for later use during a numerical simulation.

4. DESCRIPTION OF TESTING PROGRAM

To understand the failure mechanism in a heterogeneous medium, a careful testing program was conducted. In total 66 specimens were tested in biaxial loading condition and in each test recognisable incidents during loading process were

Table 2. Summary of physical and mechanical properties of four model materials used

Model material designation	SG	γ_d (g/cm^3)	n (%)	σ_c (MPa)	σ_c/σ_Q	E (GPa)	E/E_Q	c (MPa)	φ ($^\circ$)	σ_t (MPa)	ν
Q	2.54	1.61	37	47.1	1.00	6.85	1.00	9.9	44.4	7.42	0.18
F	2.54	1.48	42	36.0	0.76	5.50	0.80	8.3	40.3	5.44	0.23
B	2.61	1.09	58	8.9	0.54	2.37	0.97	2.2	37.3	2.07	0.23
P	2.13	1.48	30	25.4	0.19	6.66	0.35	6.1	38.9	5.55	0.24

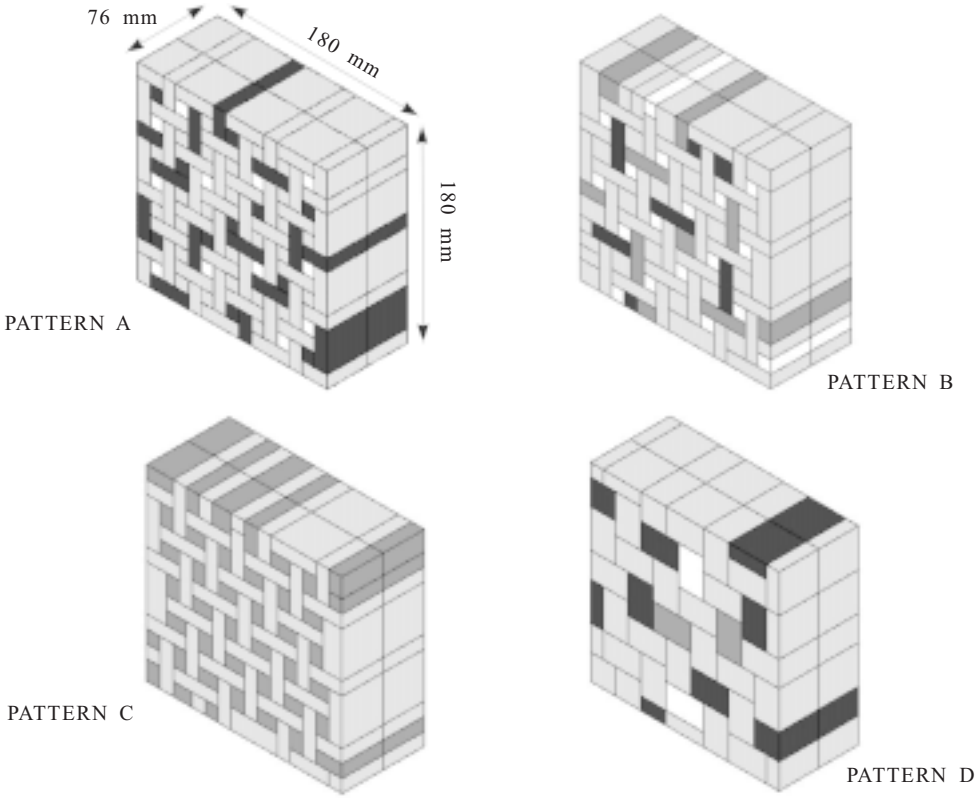

Figure 4. Perspectives of four systematic patterns (A, B, C, and D) used to simulate natural textures[12]. Black: Q, dark gray: P, light gray: F, and white: B.

recorded along with load level and proper photographs, which were made using a digital camera. To perform biaxial testing on specimens the 1000 kN True Triaxial Machine (TTS) developed in IIT Delhi by Rao and Tiwari[11] was used, but in the biaxial frame of that one pair of hydraulic jacks were removed to get sufficient space for online photography during loading process.

4.1 Specimen Geometry

Intricate interlocking patterns of crystalline rocks at micro-level were partly simulated into four different simple systematic patterns at macro-level[12] i.e., pattern-A, B, C, and D (Fig. 4). In all patterns the overall size of specimen is 180 mm × 180 mm × 76 mm. It is made of two layers, each having 38 mm thickness. Each layer is made of dissimilar element sizes interlocked together. The building elements for specimens were prepared by mixing of dental plaster with different distilled water ratios and then pouring the paste into split moulds.

4.2 Testing of Specimens

After preparation, each specimen was carefully put in the loading chamber of the biaxial testing machine (Fig. 5). To ensure a friction free loading, 0.5 mm thick pairs of Teflon sheets were put on

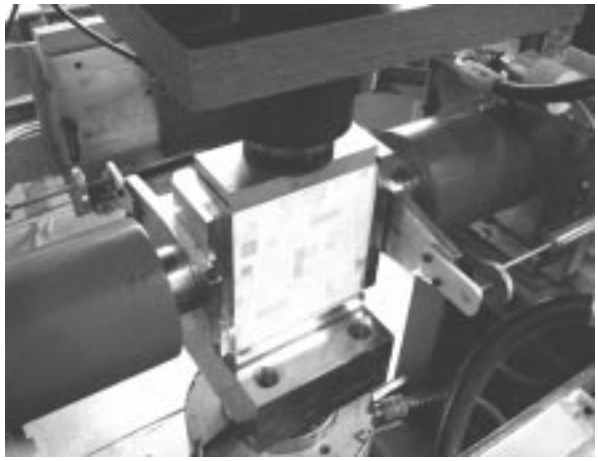

Figure 5. Final large specimen in the loading section of TTS.

four faces of the specimens. After applying certain amount of lateral load, the axial load was gradually increased up to failure and a little further to ensure that specimen has failed.

Very low strain rate was selected to provide sufficient time to observe and record cracking processes in the sample faces and to make photographic recording. Each test took around 30-45 min to complete. In total 66 specimens were tested at four lateral pressures, i.e., 0.08 MPa, 0.15 MPa, 0.88 MPa, 3.1 MPa, four interlocking patterns and in each pattern with different configuration of element types.

In order to assess the effect of elemental size, a separate study was conducted on pattern *D* specimens at 0.15 MPa and 0.88 MPa. After completion of each test, specimen was carefully removed from the testing pedestal for detailed observation. Induced cracks on all six faces of specimens were mapped on printed sheets.

5. FAILURE MECHANISM

The observations during loading process show that as load increases, growing number of tensile cracks develop almost parallel to σ_1 (Fig. 6). This crack growth continues, but because of little inclination in the orientation of tensile cracks some minor shear movements occur along them. These minor shear movements are however very critical in localising damage at some points in the specimen where new

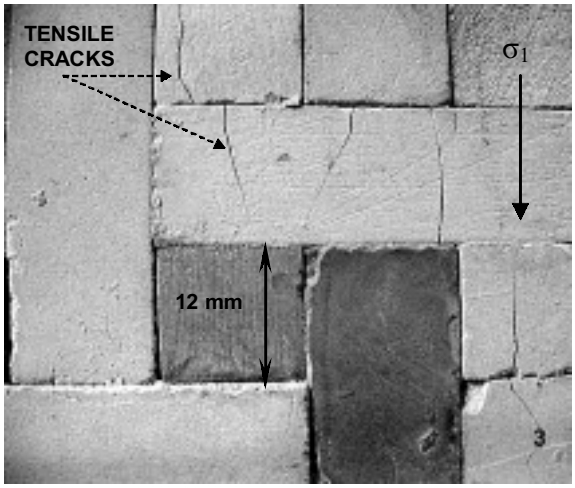

Figure 6. Crack initiation from element boundaries parallel to σ_1.

cracks develop parallel to the existing ones and therefore tiny slender columns of rock form in between. At a critical density of tensile cracks, which may happen at one or more locations of sample face, these slender tensile columns get sheared subsequently (Fig. 7).

Figure 7. Shearing fracture passing through a series of tensile cracks.

This breakage may be of bending (due to curved shape of tensile cracks) or shear nature (due to local shear forces). This incident marks an important point in failure process of rock, since it begins a series of accelerative unstable shear activities that leads to the final collapse of sample. Before this point, cracking is almost of tensile nature and after that it is mainly of shear type. In other words, crack coalescence starts at this point owing to small shear cracks, which successively join the pre-existed tensile cracks and thereby form the final failure surface.

6. STRESS-STRAIN CURVES

For each specimen, the deformational behaviour is determined through plotting its stress-strain curve under biaxial loading condition. One such curve is observed in Fig. 8 that depicts the axial and lateral stress-strain curves for specimen no. A/QFB1/0.15. This specimen is an A-pattern interlocked assembly of three different element types, i.e., *Q*, *F* and *B* with respective 22 per cent, 73 per cent and 5 per cent of each component. The specimen is tested under 0.15 MPa lateral pressure.

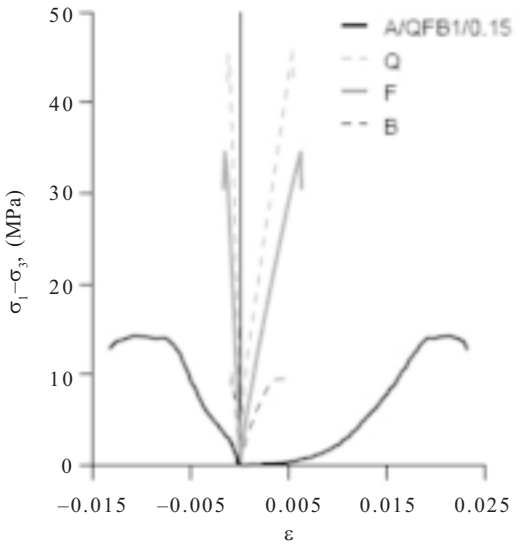

Figure 8. Deformational behaviour of specimen no. A/QFB1/ 0.15 in comparison to its constituent's behaviours.

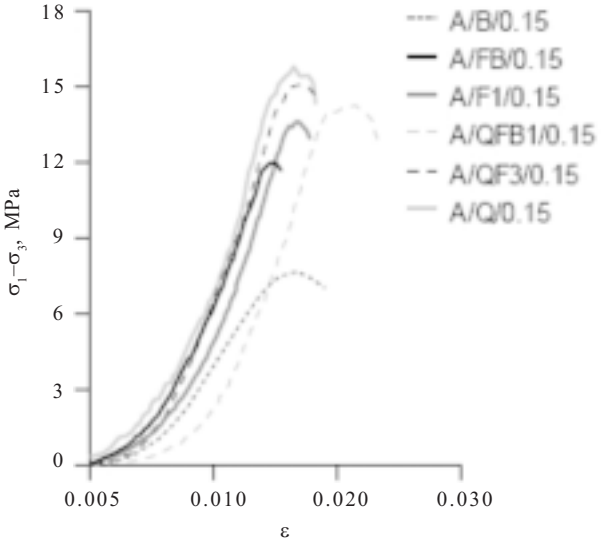

Figure 9. Stress-strain curves of six different specimens in the pattern-A.

As seen in the Fig. 8, the axial stress-strain curve exhibits an initial large strain, which is probably due to poor arrangement of some elements in the specimen that diminishes as little load is applied. Also for comparison, the stress-strain curves of three intact building elements, i.e., *Q*, *F*, and *B* are drawn in Fig. 8. Considering the peak strength, stress-strain curves for *Q* and *F* elements stand above while *B* curve stands below the stress-strain curve of interlocked specimen. This suggests that the strength of the interlocked specimen is reduced due to the interlocking pattern itself, but is affected by the strength of the major constituent, i.e., the *F* material.

Considering the elastic modulus all three intact curve stands above the specimen curve, with *B* curve standing relatively the closest. This suggests that the elastic modulus of an interlocked material reduces drastically by the interlocking pattern, as similar to the strength condition, but is affected by the modulus of the weakest constituent as well.

To study the effect of each constituent on the overall behaviour of an interlocked specimen, the stress-strain curves of the six specimens are drawn together in the Fig. 9. All theses specimens belong to the A-pattern category, but the number and percentages of the constituents differ amongst them. It is observed in this figure that the specimen with the *B* element only, has the lowest curve whereas the one with the *Q* element only has the highest curve. In between these two extremes, stand the curves of mixed specimens with the specimens having greater percentages of *Q* or *F*, at the higher position. The detail information about peak strength and elastic modulus of all the six specimens is given in Table 3.

7. APPLICATION OF DISTINCT ELEMENT METHOD (DEM)

To further study the controlling parameters in the brittle failure, a numerical study is performed based on the DEM and using the UDEC software by ITASCA Consulting Group, Inc. The Universal

Table 3. Strength and elastic modulus of six different specimens in the pattern-A

Specimen	Components (%)	σ_1 (MPa)	*E* (MPa)
A/B/0.15	QFB: 0/0/100	7.9	768
A/FB/0.15	QFB: 0/95/5	12.4	1198
A/F1/0.15	QFB: 0/100/0	13.9	1385
A/QFB1/0.15	QFB: 22/73/5	14.5	1387
A/QF3/0.15	QFB: 35/65/0	15.3	1618
A/Q/0.15	QFB: 100/0/0	16.0	1754

Distinct Element Code (UDEC) is a two-dimensional numerical program based on the DEM for discontinuum modelling.

By means of UDEC, effect of geometrical heterogeneity on macroscopic properties of an interlocked heterogeneous system is investigated in detail besides the experimental study. A size study is carried out, but two original investigations that were not easily practical in the laboratory are performed in addition.

7.1 Element Size

Using UDEC, one series of real specimens used in the experimental size study are simulated. This study is performed on pattern *D* specimens at 0.15 MPa lateral pressure. Model results, according to Figs 10 and 11, follow the experimental results but with less incongruity, allowing for fitting of proper trend lines. In case of peak strength dependency on element size, Fig. 10, results are closely following the famous Hall-Petch Law[13,14] in the following form:

$$\sigma_c = 9.0 + \frac{49.7}{\sqrt{D}} \qquad (3)$$

where k_y = 49.7 and σ_0 = 9.0 MPa.

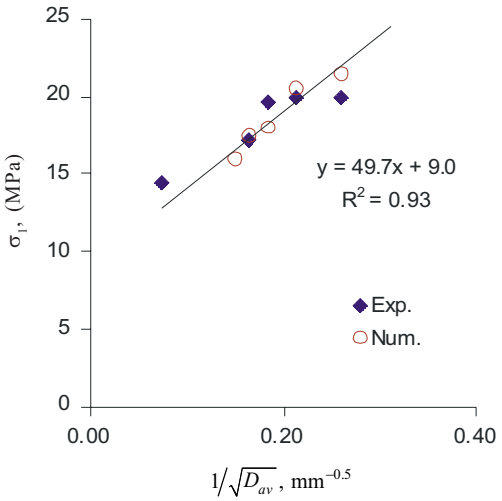

Figure 10. Effect of element size on σ_1 at 0.15 MPa lateral pressure.

The size influence on overall elastic modulus and modulus ratios of numerical specimens is presented in Fig. 11. Resembling experimental results, and in contrast to strength, there are continuous drops in modulus and modulus ratio of specimens at smaller sizes.

7.2 Size Heterogeneity

Size heterogeneity at this point refers to the presence of two different element sizes in a system of interlocked elements. The difference between two sizes present in the system (ΔD_{av}) is considered as an index for the size heterogeneity. By varying this parameter, its effect on strength of an interlocked system is investigated.

Sixteen biaxial tests are performed numerically at different values of ΔD_{av} and related results about strength are given in Fig. 12(a). According to Fig. 12(a), increase of size heterogeneity (ΔD_{av})

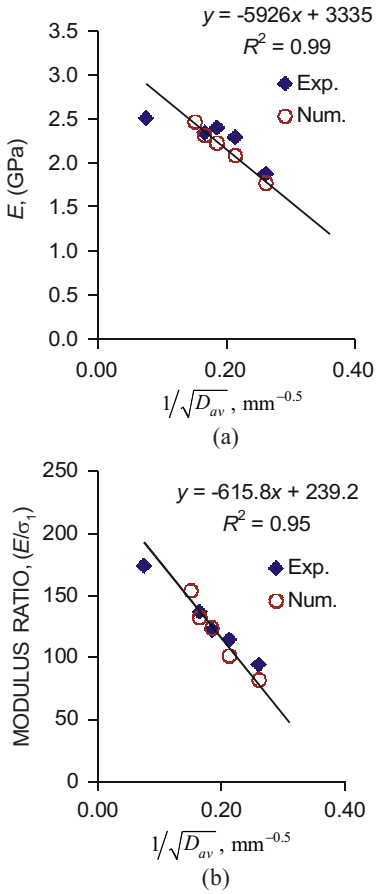

Figure 11. Effect of element size on: (a) elastic modulus and (b) modulus ratio at 0.15 MPa lateral pressure.

causes reduction in overall strength of the system. As ΔD_{av} increases, large elements become larger and small elements become smaller. As concluded in previous section, larger elements cause strength reduction and smaller elements result in higher strength, therefore, the overall reduction of strength at higher values of ΔD_{av} entails that the influence of larger elements is greater than smaller elements in an interlocked system.

7.3 Length Ratio

Length ratio (L_{max}/L_{min}) is defined as the ratio between length of the longest element to the width of narrowest element in the specimen. Role of this factor on overall macroscopic properties of an interlocked system is thus studied using numerical specimens of pattern-*D*.

In Fig. 12(b) the role of length ratio on overall strength is depicted. As seen in this figure length ratio has a negative effect on strength but the destructive role decreases at large values of length ratio. This effect is given more explicitly in the form of following formula that is the best fit to the data points in Fig. 12(b)

$$\sigma_1 = -5.34 \times \ln\left(\frac{L_{\max}}{L_{\min}}\right) + 23.70 \qquad (4)$$

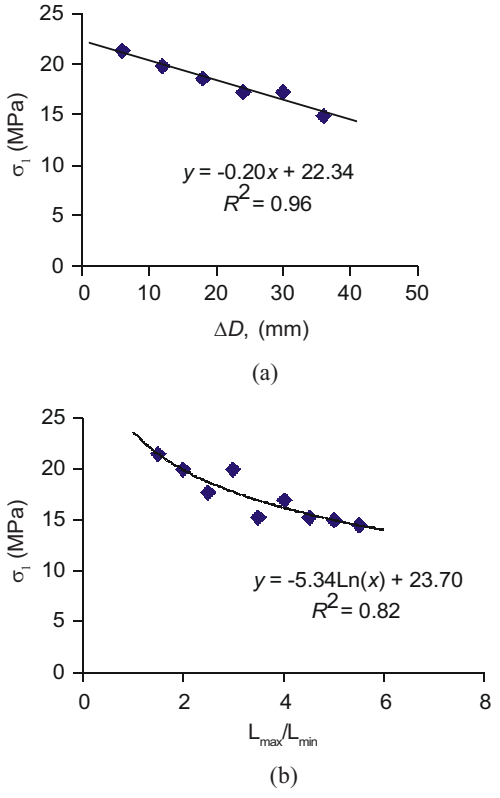

Figure 12. Effect of (a) size heterogeneity and (b) length ratio of elements on overall strength.

8. APPLICATION OF BEAM AND BUCKLING THEORIES TO BRITTLE FAILURE

Based on detailed experimental observations it became clear that the brittle failure is primarily a continuous tensile cracking process. At a critical density of tensile cracks, tiny slender columns of rock formed in between of tensile cracks buckle. This begins a series of unstable shear activities that leads to the final collapse of sample. Considering the geometry of the problem, as shown in Fig. 13, and using classical beam and buckling theories, a new criterion is derived for uniaxial compressive strength of crystalline rocks

$$\sigma_c = \frac{10K\sigma_{tm} + 9E_m}{\left(2493 + \frac{346}{K}\left(\frac{E_m}{\sigma_{tm}}\right)^{1.70}\right)^{0.38} + 10.5} - 142.5\frac{\sigma_{tm}}{E_m} \qquad (5)$$

where, K is the interlocking factor of minerals/grains/crystals, a new parameter, E_m is the average elastic modulus of rock minerals, and σ_{tm} is the average tensile strength of rock minerals.[15]

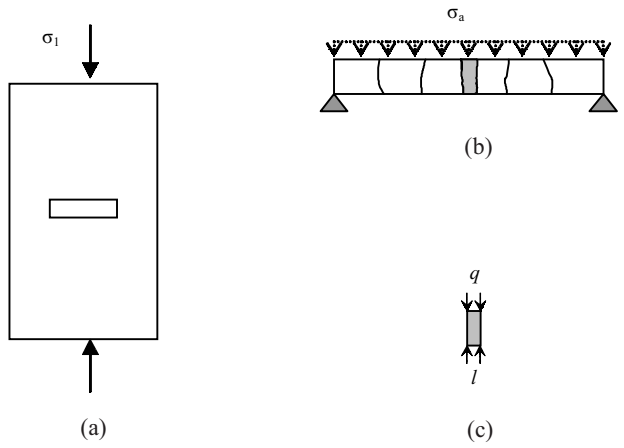

Figure 13. Schematic view of (a) a specimen under compression, (b) a beam element in the sample under induced bending pressures, σ_a, and (c) a tiny column having length of *l*, under buckling stress, *q*.

The above formula is the short form developed via MATLAB after the original formula, which was very complicated and lengthy, thus the equation is valid in the following domains only:

$1 \text{ GPa} < E_m < 200 \text{ GPa}$

$10 \text{ MPa} < \sigma_{tm} < 500 \text{ MPa}$

$0.0001 < K < 5$

From the three parameters in the Eqn (5), the K is a new parameter that quantifies the interlocking properties of rock minerals. To calculate K for a rock, knowing the average values of E_m, σ_{tm} and σ_c for that rock, the Eqn (5) could be used in the reversed order.

9. CONCLUSIONS

Brittle failure starts with tensile microcracks extending parallel to the major principal stress. These microcracks later increase in density rather than length along with increase in s1 till the elastic limit. Somewhere around this point tiny slender columns formed in between microcracks in heavily cracked regions break due to buckling or local shear forces triggering a subsequent accelerative series of shear activities in sample that finally leads to complete failure.

The deformational behaviour of interlocked specimens is studied under biaxial loading condition. Comparing with the stress-strain curves of the constituent model materials, it is concluded that the interlocking pattern itself drastically reduces the brittleness of the specimens. Presence of considerable amount of stronger elements strengthens the specimens, whereas the little amount of weaker elements causes immediate reduction of elastic modulus.

Distinct element modelling is used and it is found that the geometrical factors, i.e., element size, size heterogeneity and length ratio, all have reducing effect on strength but an increasing effect on elastic modulus and modulus ratio of the heterogeneous crystalline rocks.

Using classical beam and buckling theories a new criterion is derived for uniaxial compressive strength of crystalline rocks that, for the first time, highlights the role of crystal interlocking on the compressive strength of rocks in a quantitative way.

REFERENCES

1. Ratajeski, K. & Glazner, A. Atlas of igneous and metamorphic rocks, minerals and textures. University of North Carolina, Chapel Hill, 2007. http://www.geosci.unc.edu/Petunia/IgMetAtlas/mainmenu.html

2. Sprunt, E.S. & Brace, W.F. Direct observation of microcavities in crystalline rocks. *Int. J. Rock Mech., Min. Sci. Geomech. Abstr.*, 1974, **11**, 139-150.

3. Barth, T.F.W. Theoretical petrology. Wiley, New York, 1952.

4. Belikov, B.P. Plastic constants of rock-forming minerals and their effect on the elasticity of rocks. *In* Physical and mechanical properties of rocks, edited by B.V. Zalesskii. Academy of Sciences of the USSR, Israel Program for Scientific Translations, Jerusalem, 1967. pp. 124-40.

5. Knittle, E. Static compression measurements of equations of state. *In* Mineral physics and crystallography: A handbook of physical constants, edited by T.J. Ahrens. American Geophysical Union Press, 1995. pp. 98-143.

6. Dorner, D. & Stöckhert, B. Plastic flow strength of jadeite and diopside investigated by microindentation hardness tests. *Tectonophysics*, 2004, **379**, 227-38.

7. Johnson, K.L. Contact mechanics, Cambridge University Press, London, 1985.

8. Bruland, A. Hard rock tunnel boring. Norwegian University of Science and Technology, Trondheim, Norway, 1998. PhD Thesis.

9. Suggested methods for determining the uniaxial compressive strength and deformability of rock materials. International Society of Rock Mechanics, 1972.

10. Suggested methods for determining the strength of rock materials in triaxial compression. International Society of Rock Mechanics, 1977.

11. Rao, K.S. & Tiwari, R.P. A polyaxial testing system for prediction of engineering behaviour of jointed rock and rock mass. *ASTM Geotech. Testing J.*

12. Noferesti, H. & Rao, K.S. Physical simulation of brittle failure in rocks. *In* Proceedings of the Indian Geotechnical Conference, December 2006, Chennai. pp. 373-76.

13. Hall, E.O. The deformation and aging of mild steel: (iii) Discussion of results. *In* Proceedings of the Physical Society of London, B64, London, 1951. pp. 747-53.

14. Petch, N.J. The cleavage strength of polycrystals. *J. Iron Steel Inst.*, 1953, **174**, 25-28.

15. Noferesti, H. Simulation of brittle failure in crystalline rocks. Indian Institute of Technology Delhi, New Delhi, 2007. PhD Thesis.

Contributors

Dr K.S. Rao is Professor in the Dept of Civil Engineering, Indian Institute of Technology Delhi. His main areas of interest are strength and deformation behaviour of rocks and rock masses, underground structures, stability of slopes, ground response, site characterisation and seismic microzonation of mega-cities. He has more than 180 research publications to his credit, received *Best PhD Thesis Professor Leonard's Award* as well as nine other best paper awards for his works. He has been coordinating several research projects in the areas of rock mechanics and earthquake geotechnical engineering.

Dr Noferesti Hossein obtained his bachelor and postgraduate degrees in Mining Engineering from the Shahroud University of Technology and Amirkasbir University, Iran. He obtained his PhD on simulation of brittle failure in crystalline rocks, from IIT Delhi in 2007. Presently, he is working as Asst Prof, Brijand University, Iran. He has published/presented some papers in national international journals and conferences.